ISSN 1063-7710, Acoustical Physics, 2016, Vol. 62, No. 5, pp. 523–531. © Pleiades Publishing, Ltd., 2016.

CLASSICAL PROBLEMS OF LINEAR ACOUSTICS AND WAVE THEORY

Wave Propagation Characteristics of Helically Orthotropic Cylindrical Shells and Resonance Emergence in Scattered Acoustic Field. Part 2. Numerical Results[1]

Majid Rajabi

Sustainable Manufacturing Systems Laboratory, School of Mechanical Engineering, Iran University of Science and Technology, Narmak, Tehran, Iran

e-mail: majid_rajabi@iust.ac.ir

Received June 19, 2014

Abstract—In the present work as the second part of the research work on wave propagation characteristics of helically orthotropic cylindrical shells, the main aim is to use the developed solution for resonance isolation and identification of an air-filled and water submerged Graphite/Epoxy cylindrical shell and quantitative sensitivity analysis of excited resonance frequencies to the perturbation in the material's elastic constants. The physical justifications are presented for the singular features associated with the stimulated resonance frequencies according to their style of propagation and polarization, induced stress-strain fields and wave type. For evaluation purposes, the wave propagation characteristics of the anisotropic shell and the far-field form function amplitude of a limiting case are considered and good agreement with the solutions available in the literature is established.

Keywords: resonance bifurcation, material characterization, sensitivity analysis

DOI: 10.1134/S1063771016050122

In order to illustrate the nature and general behaviour of the solution, we consider some numerical examples. Our particular example is a Graphite/Epoxy (AS4/3501-6) helically filament wound composite cylindrical shell submerged in water and filled with air at atmospheric pressure and ambient temperature with their physical properties as given in the table. As it is concluded from the given material properties, the transversely isotropy condition governs for the present unidirectional orientation fiber-reinforced composite material; i.e. equivalent properties in isotropy *ts*-plane: $E_t = E_s$, $G_{lt} = G_{ls}$, $\nu_{lt} = \nu_{ls}$ and $G_{ts} = 0.5E_t / (1 + 2\nu_{ts})$. Notice that our proposed solution is organized for general monoclinic condition of anisotropy.

A MATLAB® code was constructed for computing the global modal transfer matrix, $\mathbf{T}_n$, considering boundary conditions, calculating the unknown total and background scattering coefficients, and ultimately, the wave propagation characteristics. All the calculations are done for a unit amplitude incident plane wave ($\varphi_0 = 1$). The computations were performed on a Pentium IV personal computer with a maximum number of sublayers $q_{\max} = 50$, and a maximum truncation constant of $n_{\max} = (ka_q)_{\max} + 15$, selected to guarantee the convergence of the solution in the high frequency range. The interested frequency range is selected as $0 \le ka_q \le 20$ with a frequency resolution of $\Delta ka_q = 0.01$, in order to make uncomplicated the developing and identification process of main resonances and to avoid the appearance of ultra-narrow resonances. Since the convergence and stability of the proposed solution is significantly dependent to the number of assumed sublayers $q_{\max}$, we need to particularly examine the steadiness of the numerical calculations as function of $q_{\max}$. Therefore, Fig. 1 shows the changes in the back-scattered form function amplitude of our Glass/Epoxy shell with thickness, $h/a_q = 0.05$, and at the maximum limit of selected frequency range, $ka_q = 20$, angle of incidence $\alpha = 5°$ for different values of maximum sublayers, $q_{\max}$. Apparently, proper convergence with the truncation error of 10^{-4} is achieved with $q_{\max} \approx 10$ and obviously, the selected value of $q_{\max} = 50$ in our numerical calculations is over satisfactory.

First of all, in order to check the overall validity of the scattering formalism, we computed the variations of the backscattering form function amplitude with dimensionless frequency for oblique incidence ($\alpha = 9°$) upon an air-filled boron/aluminum unidi-

[1] The article is published in the original.

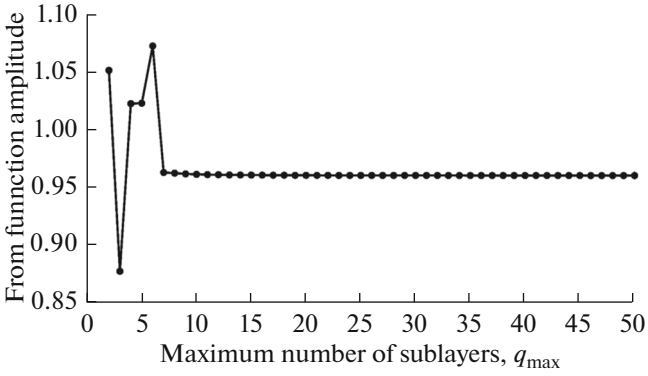

Fig. 1. The changes in the backscattered form function amplitude of Glass/Epoxy shell with thickness of $h/a_q = 0.05$, and at the maximum limit of selected frequency range, $ka_q = 20$, and at angle of incidence, $\alpha = 5°$, for different values of maximum sublayers, $q_{\max}$.

rectional composite cylindrical shell submerged in water by setting $h/a_q = 0.16$, $\rho_c = 2738$ kg/m^3, $c_{11} = c_{22} = 142.1$ GPa, $c_{12} = 71.1$ GPa, $c_{13} = c_{23} = 66.4$ GPa, $c_{33} = 219.4$ GPa, $c_{44} = c_{55} = 37.1$ GPa, $c_{66} = 35.5$ GPa, $\rho_1 = 1000$ kg/m^3, $c_1 = 1469$ m/s, $\rho_2 = 1.2$ kg/m^3 and $c_2 = 340$ m/s in our general MATLAB® code. The numerical results, as shown in Fig. 2a show good agreement with those displayed in Fig. 7a in [1]. For further check, we computed the wave propagation characteristics associated to the dipole mode of vibration ($n = 1$) of a monoclinic cylindrical shell with normalized thickness as $h/a_q = 0.261$, normalized material properties as $E_l/E_t = E_l/E_s = 40$, $G_{lt}/E_t = G_{lt}/E_t = 0.6$, $G_{tt}/E_t = G_{ss}/E_t = 0.5$, $\nu_{lt} = \nu_{ls} = 0.25$ and filament angle $\phi = 45°$. For this purpose, we used our general formulation to determine the wave propagation characteristics by setting the determinant of the coefficient matrix in Eq. (21) of part 1 [2] equal to zero, i.e., $\left|\mathbf{\Lambda}_n^+\right| = 0$, and searching for its frequency roots. Figure 2b shows excellent agreements between the computed normalized modal frequencies, $\Omega = \omega(a+b)\sqrt{\rho_c/G_{lt}}/2\pi$, as a function of dimensionless axial wave length, $k_z h/\pi$, with those displayed in Fig. 1 of Ref. [3].

Figure 3 shows the wave propagation characteristics (i.e., dispersion curves: dimensionless frequency, ka_q, with respect to the dimensionless axial wavelength, $k_z a_q$) of an air-filled and water submerged Graphite/Epoxy cylindrical shell with $h/a_q = 0.05$ thickness and the filament angle $\phi = 45°$, for selected mode numbers $n = 2$ (Fig. 3a) and $n = 5$ (Fig. 3b), respectively, in the dimensionless frequency range of $0 < ka_q < 20$. The resonance branches associated to partial waves on the anisotropic cylindrical body are observed. The resonance branches associated to helically circumnavigating resonances are designated by the integers (n,l) where n specifies the fundamental mode number and the second, $l = 1, 2, 3, \ldots$, is to identify the overtones associated with the fundamental mode of the vibration. The superscripts "+" and "–" refer to the anticlockwise and the clockwise types of circumnavigating, respectively. As it is seen, an interesting bifurcation phenomenon is emerged in frequency spectra as the axial wave number k_z takes non-zero values; e.g., the resonance spectra of $(2,1)^-$and $(2,2)^+$, $(2,3)^+$ and $(2,4)^-$, $(5,1)^-$ and $(5,2)^+$ are branched from identical frequencies for which an entirely circumnavigating type of wave propagation (i.e., zero helix angle, $\Psi = 0$) is anticipated. This observed splitting behavior is interpreted in this way that for the cases of a zero helix angle, both clockwise and anti-clockwise propagating partial waves experience a symmetric condition with respect to the elasticity of the cylindrical structure; but for the non-zero helix angles, both of the wave propagation types meet different states of the material effective elasticity.

Before we start the resonance classification and identification process for the current scattering problem, it would be helpful to present a brief review on the concepts in Resonance Acoustic Theory (RST). Considering the exposed physics associated to the scattering phenomena from RST, we know that the scattered acoustic field from the targets consists of resonance spectra superimposed on relatively flat background which can be attributed to the target material density and geometrical parameters. The resonance spectra is a cumulative of the excited resonances of the target linked to the constructive interference of propagating surface waves making multiple encirclements of body's periphery due to the phase matching phenomenon. The surface waves are launched from the strike points on the object boundary and travel over the body in spiral or helical trajectories, depending to the incident angle. In the case of the normal incidence, the waves travel in entirely circumnavigating trajectories and for the oblique incidence, the waves travel in helical ones making helix angle which depends on their corresponding phase velocity of propagation [4, 5] (i.e., the helix angle, $\Psi = \tan^{-1}(k_z a/n)$, and the phase velocity, $c_{\rm ph} = \omega/\left[k_z^2 + (n/a)^2\right]^{1/2}$, are simply related as $\Psi = \tan^{-1}\left\{\left[(\omega a/nc_{\rm ph})^2 - 1\right]^{1/2}\right\}$ where $k_z = k\sin\alpha$).

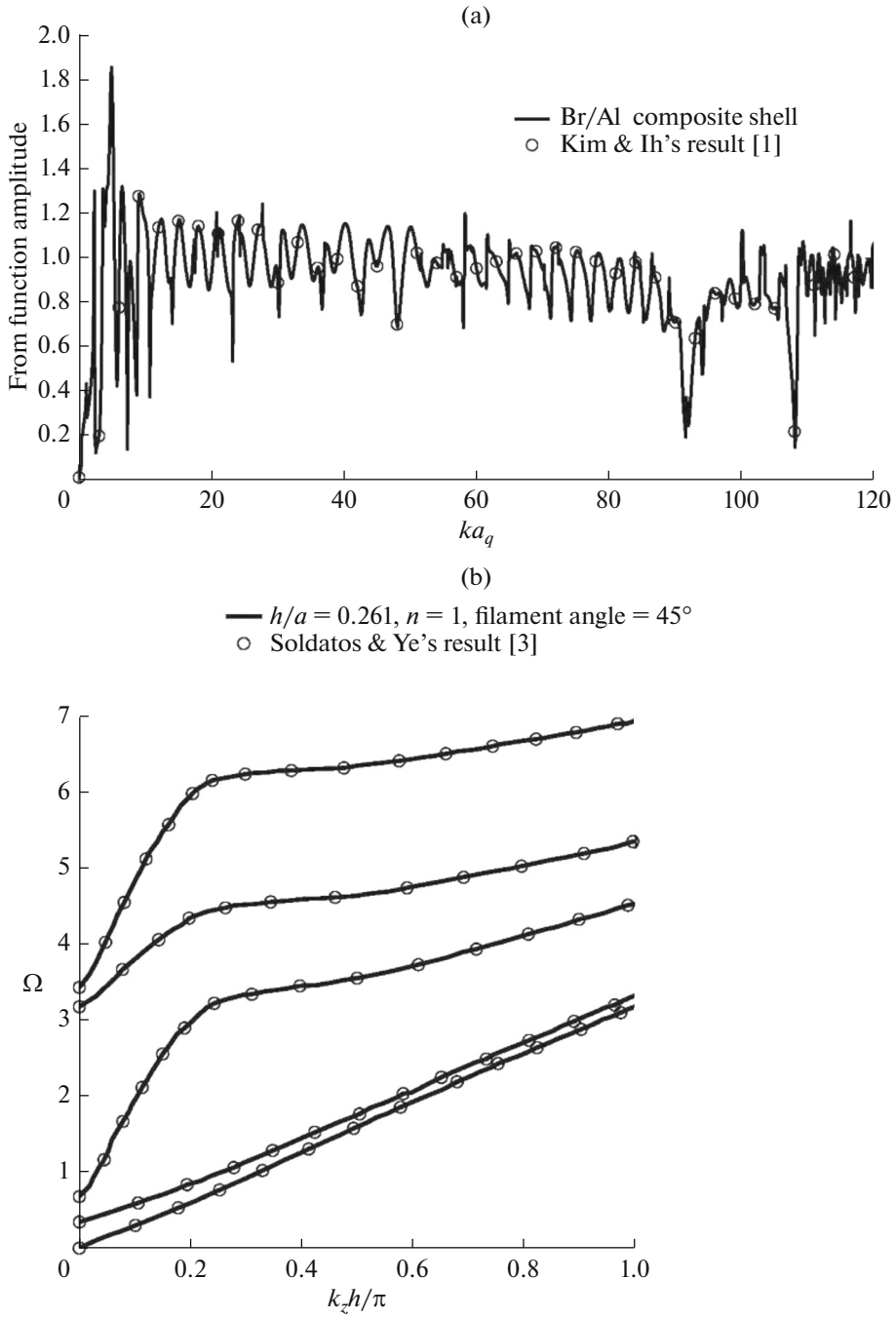

Fig. 2. (a) The variations of the backscattering form function amplitude with thickness $h/a_q = 0.16$, dimensionless frequency for oblique incidence, $\alpha = 9°$, upon an air-filled boron/aluminum unidirectional composite cylindrical shell submerged in water compared with the results of Kim and Ih [1]. (b) The wave propagation characteristics associated to the dipole mode of vibration, $n = 1$, of a monoclinic cylindrical shell with normalized thickness as $h/a_q = 0.261$, normalized material properties as $E_l/E_t = E_l/E_s = 40$, $G_{lt}/E_t = G_{lt}/E_t = 0.6$, $G_{tt}/E_t = G_{ss}/E_t = 0.5$, $\nu_{lt} = \nu_{tt} = 0.25$ and filament angle $\phi = 45°$, compared with the results of Soldatos and Ye [3].

The special case of the normal insonification; i.e., $\alpha = 0°$, may represent special features which distinguish the monoclinic cylindrical body from the lower anisotropy cases (e.g., isotropic, transversely isotropic, orthotropic). The non-trivial solution of the problem, Eq. (4) of part 1 [2], reduces to

Physical properties of the fluid and solid media

Water	$\rho_1 = 1000\ \mathrm{kg/m^3}$, $c_1 = 1480\ \mathrm{m/s}$
Air	$\rho_2 = 1.2\ \mathrm{kg/m^3}$, $c_2 = 340\ \mathrm{m/s}$
AS4/3501-6 Graphite/Epoxy	$\rho_c = 1600\ \mathrm{kg/m^3}$, $E_l = 138\times10^9\ \mathrm{N/m^2}$, $E_t = E_s = 8.9\times10^9\ \mathrm{N/m^2}$, $G_{ts} = 2.89\times10^9\ \mathrm{N/m^2}$, $G_{lt} = G_{ls} = 5.17\times10^9\ \mathrm{N/m^2}$, $\nu_{ts}=0.54$, $\nu_{lt} = \nu_{ls}=0.3$

$$\mathbf{Y} = \begin{Bmatrix} u_z \\ u_\theta \\ u_r \\ \sigma_{rr} \\ \sigma_{r\theta} \\ \sigma_{rz} \end{Bmatrix} = \sum_{n=0}^{\infty} \begin{Bmatrix} a_q w_{z,n}(\eta)\ \sin(n\theta) \\ a_q w_{\theta,n}(\eta)\ \sin(n\theta) \\ a_q v_{r,n}(\eta)\ \cos(n\theta) \\ c_{44}\Sigma_{rr,n}(\eta)\ \cos(n\theta) \\ c_{44}\Gamma_{r\theta,n}(\eta)\ \sin(n\theta) \\ c_{44}\Sigma_{rz,n}(\eta)\ \cos(n\theta) \end{Bmatrix} e^{-i\omega t}, \qquad (1)$$

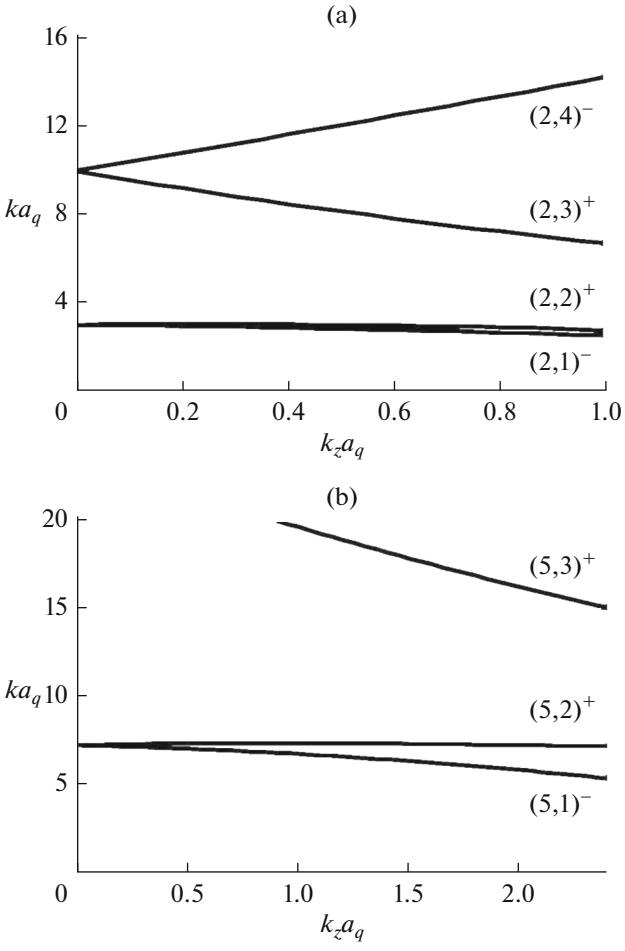

Fig. 3. The dispersion curves (frequency spectra) associated to an air-filled and water submerged Graphite/Epoxy cylindrical shell with $h/a_q = 0.05$, filament wound angle $\phi = 45°$, for selected mode numbers $n = 2$ (a) and $n = 5$ (b).

It could be easily found out that there is no contribution of c_{31}, c_{32}, c_{33} and c_{34} in the dynamics of the body or in a simple word, $\varepsilon_{zz} = 0$, $\sigma_{zz} = 0$, which along with $k_z = 0$, implies that there is no wave propagation (guided waves) along the z-axis, but the existence of u_z and $\partial u_z/\partial\theta$ indicates the polarization of circumnavigating wave motions along the z-axis. In comparison with the case dealing with isotropic, transversely isotropic and orthotropic cylindrical structures, the normal insonification of a generally monoclinic cylindrical shell leads to a non-zero value and asymmetric pattern of the axial component of the displacement vector; i.e., $u_z = \sum_{n=1}^{\infty} a_q w_{z,n}(\eta)\ \sin(n\theta) \neq 0$. In addition to the above wave polarization analysis, a practical note comes into mind that in the non-destructive evaluation of a generally monoclinic anisotropic cylindrical structure, the oblique incidence is essential to take into account all the elements of the stiffness matrix, [6, 7].

Figure 4 illustrates the variation of the modal form function amplitude, the modal background scattering amplitude and the isolated modal resonance scattering amplitude (which is obtained from the subtraction of the modal background component from the modal form function spectrum) of an air-filled and water submerged Graphite/Epoxy cylindrical shell with $h/a_q = 0.05$, filament angle $\phi = 45°$, at the angle of incidence $\alpha = 5°$, with respect to dimensionless frequency, ka_q, for selected mode numbers $n = 2$ (Fig. 2a) and $n = 5$ (Fig. 2b), respectively. As it is clear in these figures, the modal scattering coefficients perfectly coincide with the inherent background coefficients, except in the resonance region where the resonances are clearly isolated. Each peak in the resonance components are associated to a certain resonance which by comparing to the intersection of dispersion curves of Figs. 5a and 5b with the scattering line of $k_z a_q = k_z a_q \sin\alpha$, leads to the identification of the stimulated resonance frequencies as $(2,1)^-, (2,2)^+, (2,3)^+, (2,4)^-$ and $(5,1)^-, (5,2)^+, (5,3)^+$.

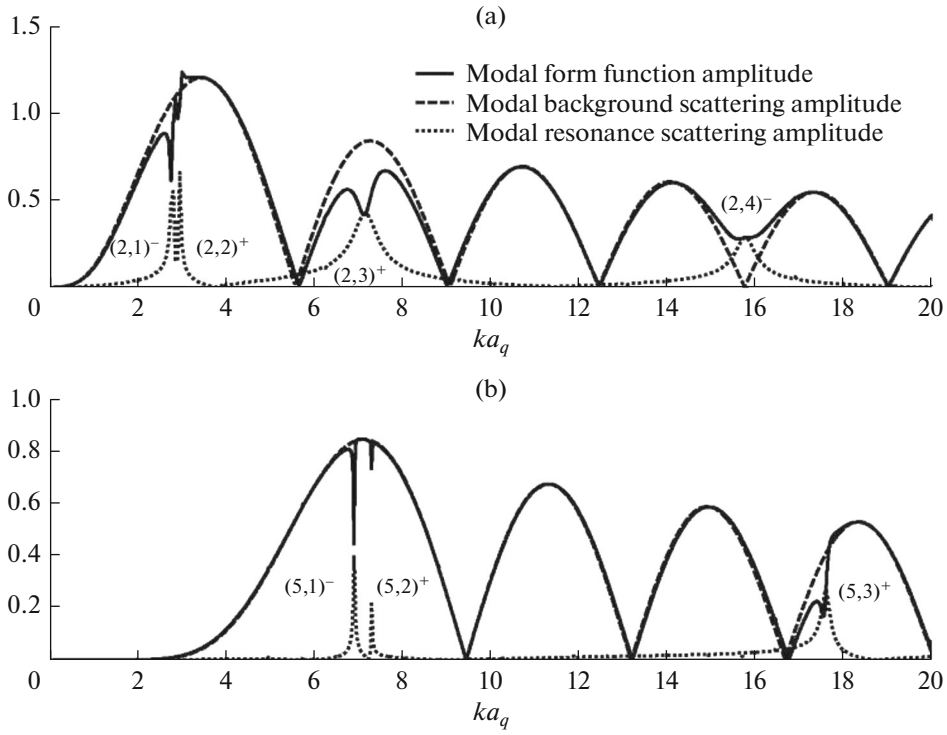

Fig. 4. The variation of the modal form function amplitude, its corresponding background scattering amplitude and the isolated resonance scattering amplitude associated to selected mode numbers $n = 2$ (a) and $n = 5$ (b), of an air-filled and water submerged Graphite/Epoxy cylindrical shell with $h/a_q = 0.05$, $\phi = 45°$, at angle of incidence $\alpha = 5°$, with respect to dimensionless frequency, ka_q.

Figure 5 depicts the back-scattered form function amplitude of mentioned example of Graphite/Epoxy cylindrical shell, at the angle of incidence $\alpha = 5°$. Following the procedure of resonance isolation, classification and identification described above, the excited resonance frequencies are labelled.

Here, our aim is to discover the attractive feature of the resonance bifurcation (doubling) which was emerged in dispersion curves of wave propagation characteristics, in the present resonance scattering problem. In this twinning process, the foundation surface waves, which have been circumnavigating the cylindrical body in both clockwise and anti-clockwise with zero helix angle for the case of the normal incidence (i.e., $k_z = 0$), begin to take helix angles with respect to the $r\theta$-plane; $\Psi^+ = \tan^{-1}([ka_q]^+_{\text{res}} \sin\alpha/n)$ for the clockwise wave propagation mode, $(n,l)^+$, and $\Psi^- = \tan^{-1}([ka_q]^-_{\text{res}} \sin\alpha/n)$ for the anti-clockwise wave propagation mode, $(n,l)^-$. Figure 6 illustrates the frequency variation of the resonance scattering amplitude corresponding to mode number $n = 2$, for selected values of the angle of incidence, $\alpha = 0°,1°,2°,3°,4°,5°$. As the incidence angle deviates from the normal insonification state, the single resonance curve, $(2,2)$, starts to divide to $(2,3)^+$ and $(2,4)^-$. For lower incident angles; i.e., $\alpha = 1°,2°$, they demonstrate an interfering frequency zone (i.e., twin resonances). For greater incident angles; i.e., $\alpha = 3°,4°,5°$, two completely separated resonance branches are observed. Figure 7 illustrates the resonance doubling phenomenon for selected mode numbers $n = 4$ (Fig. 7a), $n = 5$ (Fig. 7b), $n = 8$ (Fig. 7c), $n = 13$ (Fig. 7d).

As mentioned before, the resonances are the fingerprints of materials, and the materials with different structure and geometry have their own set of resonances. For material characterization or on-line monitoring applications, these resonances are used to evaluate the various properties of the cylindrical structures by solving the inverse acoustic problem or organizing a numerical inverse model; however, it is important to categorize the resonances which show a sensitive behavior with regard to the parameter that is to be evaluated or monitored. Here, a quantitative sensitivity analysis is presented for the case of $h/a_q = 0.05$ Graphite/Epoxy cylindrical shell at oblique incidence $\alpha = 5°$, whose resonances are identified in Fig. 5. To

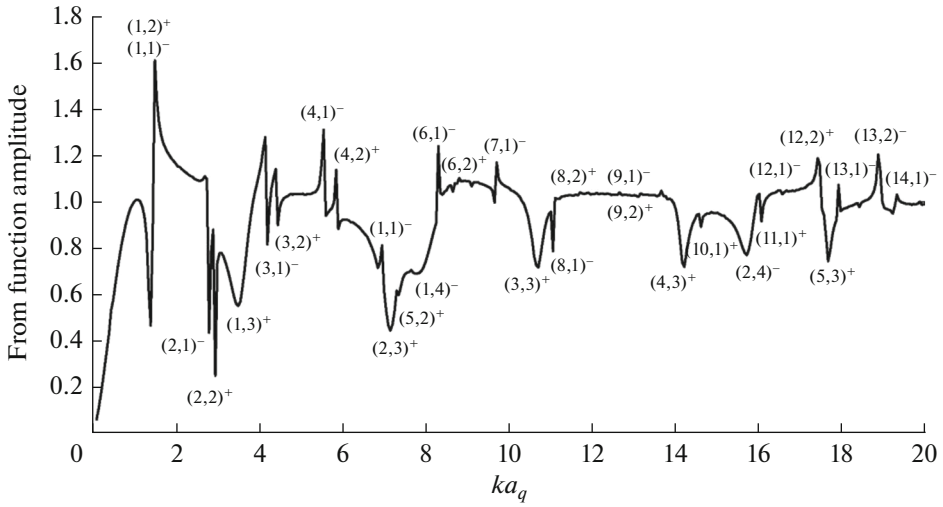

Fig. 5. The normalized backscattered form function amplitude of an air-filled and water submerged Graphite/Epoxy cylindrical shell with $h/a_q = 0.05$ thickness, $\phi = 45°$, excited at angle of incidence $\alpha = 5°$. The resonance frequencies are isolated and identified according to their fundamental mode, overtone number, direction of corresponding propagating wave mode.

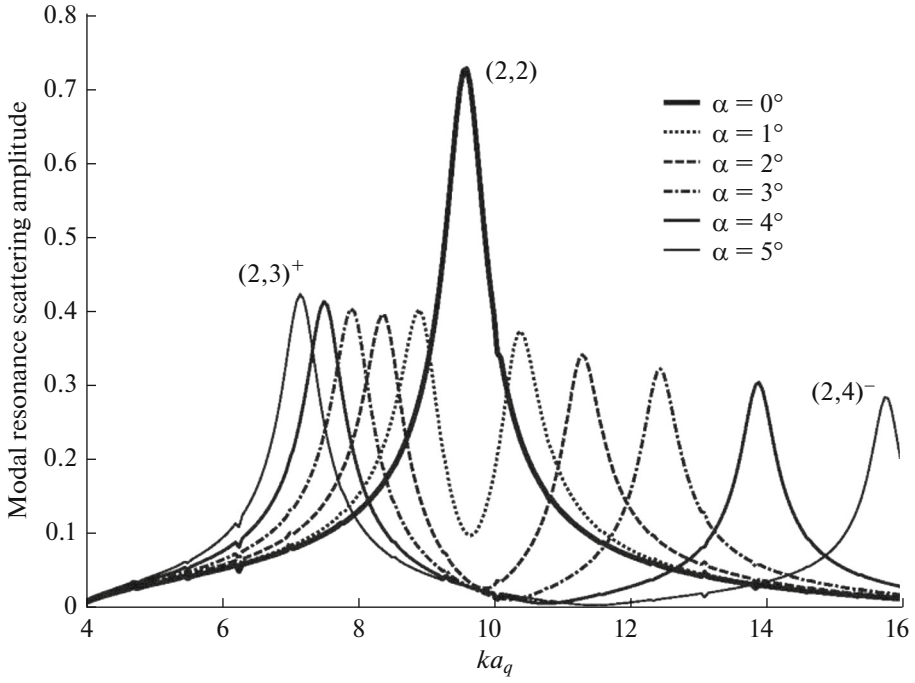

Fig. 6. The frequency variation of the resonance scattering amplitude corresponding to a selected resonance mode $n = 2$, of an air-filled and water submerged Graphite/Epoxy cylindrical shell with $h/a_q = 0.05$ thickness, filament angle $\phi = 45°$, for selected of incident angle, $\alpha = 0°, 1°, 2°, 3°, 4°, 5°$.

do this, the main independent fiber-reinforced composite material constants, $E_l, E_t, G_{lt}, \nu_{lt}$ and G_{ts} are perturbed so that the first signatures of variations are detected. The dimensionless sensitivity parameter is defined as $(\delta ka_q/ka_q)/(\delta P/P) \times 100\%$ which means the percentage of the normalized shift in the resonance frequency with respect to the normalized perturbation in the objective parameter. Figure 8 displays the sensitivity parameter of the main stimulated resonance frequencies in Fig. 5 with respect to parameters E_l (Fig. 8a), E_t and E_s (Fig. 8b), G_{lt} and G_{ls} (Fig. 8c),

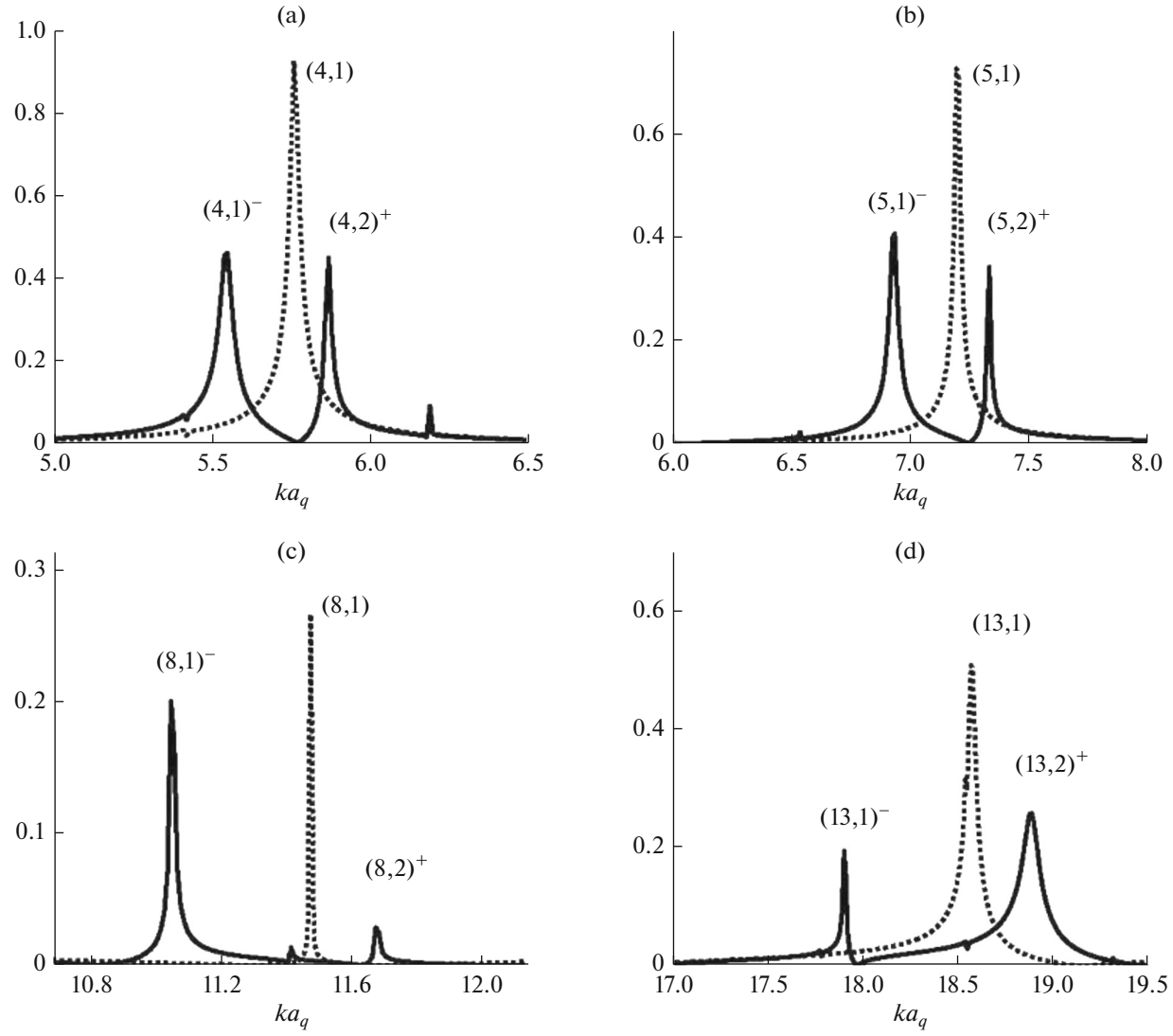

Fig. 7. The resonance doubling phenomenon for the selected mode numbers $n = 4$ (a), $n = 5$ (b), $n = 8$ (c), $n = 13$ (d) of an air-filled and water submerged Graphite/Epoxy cylindrical shell with $h/a_q = 0.05$ thickness, filament angle $\phi = 45°$.

ν_{lt} and ν_{ls} (Fig. 8d), respectively. The most important observations are stated in the following: considering the fact that an exact physical interpretation associated to each emerged feature may need to the analysis of the stress-strain polarization, displacement field imaging, and the wave propagation characteristics associated to each resonance mode of vibration. Therefore, only some practical observations are presented here. It is noteworthy that any variation of the resonance frequencies is physically related to the variation of the corresponding phase velocities of the resonances which are affected by the perturbation of material constants.

Figure 8a examines the sensitivity parameter with respect to the perturbation of E_l. This figure shows the sensitivity of the 3rd and particularly the 4th overtones of the stimulated resonance modes, $(n,l = 3,4)$, despite to indifferent behavior of the 1st and 2nd overtones of all resonance modes with respect to the perturbation of E_l. In spite of the effects associated to the perturbation in E_l, Figure 8b illustrates the sensitive manner of the 1st and particularly the 2nd overtones of the resonance modes, $(n,l = 1,2)$, with respect to variations in $E_t = E_s$, and in addition, the indifferent behavior of the 3rd and particularly the 4th overtones. The paradoxical behavior of the 1st and 2nd overtones of the resonance modes may lead to this conclusion that the excitation of these resonance branches are more affected by the generally orthotropic material property in the *s*-direction. In other words, they are sensitive to E_s rather than to E_t or E_l. For the case of

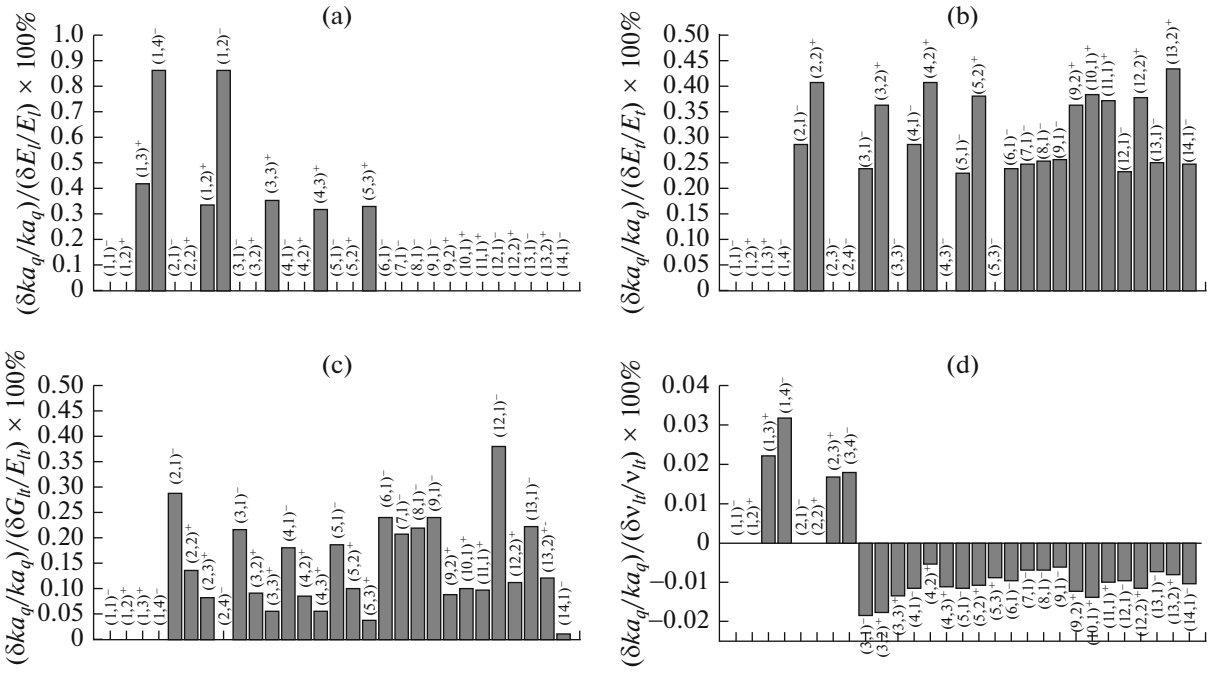

Fig. 8. The dimensionless sensitivity of resonance frequencies with respect to material elastic constants, $(\delta ka_q/ka_q)/(\delta P/P) \times 100\%$, of an air-filled and water submerged Graphite/Epoxy cylindrical shell with $h/a_q = 0.05$ thickness, filament angle $\phi = 45°$, with respect to variations of $P = E_l$ (a), $P = E_t$ and E_s (b), $P = G_{lt}$ and G_{ls} (c), $P = \nu_{lt}$ and ν_{ls} (d).

a perturbation in $G_{lt} = G_{ls}$ as shown in Fig. 8c, all resonance modes are rather susceptible which indicates that these resonance modes belong to the propagation of a shear type wave. In general, the lower overtones illustrate greater sensitivity for each resonance mode (e.g., 0.28% for $(2,1)^-$, 0.13% for $(2,2)^+$, 0.08% for $(2,3)^+$ and less than 0.01% for $(2,4)^-$). Considering the fact that one of the main differences between the overtones of a specific resonance mode is the difference between their helix angle of propagation, which gets greater values for higher overtones (i.e., as ka_q increases for higher overtones, $\Psi = \tan^{-1}(ka_q \sin\alpha/n)$ increases as well), it is roughly concluded that for the mentioned $\phi = 45°$ filament angle composite cylindrical body, the shear moduli, G_{lt} and G_{ls}, are more influential for the completely circumnavigating wave propagation modes. In a simple word, as the wave trajectories deviate from the $r\theta$-plane, the effect of G_{lt} and G_{ls} becomes smaller. Despite the sensitivity of resonance frequencies with respect to the shear moduli G_{lt} and G_{ls}, the variations of G_{ts} (i.e., between the large range of $10^4 G_{ts}$ to $10^{-4} G_{ts}$) has no effect on the resonance frequencies. Considering that G_{ts} only appears in c_{55}, c_{56} and c_{66} elements of the stiffness matrix of the mentioned example of $\phi = 45°$ filament wound cylindrical structure (i.e., $c_{55} = c_{66} = (G_{lt} + G_{ts})/2$, $c_{56} = (G_{ts} - G_{lt})/2$), where these elements affect the $r\theta$- and rz-stress and strain components, this singular feature along with the above observations lead to this conclusion that the shear type wave propagation along the mentioned anisotropic cylindrical shell is polarized mainly in the principal θz-plane, as is schematically shown in Fig. 9. Eventually, the effects associated to the variations of $\nu_{lt} = \nu_{ls}$ on the resonance frequencies are studied in Fig. 8d. As this figure displays, the 3rd and 4th overtones of the dipole ($n = 1$) and quadru-

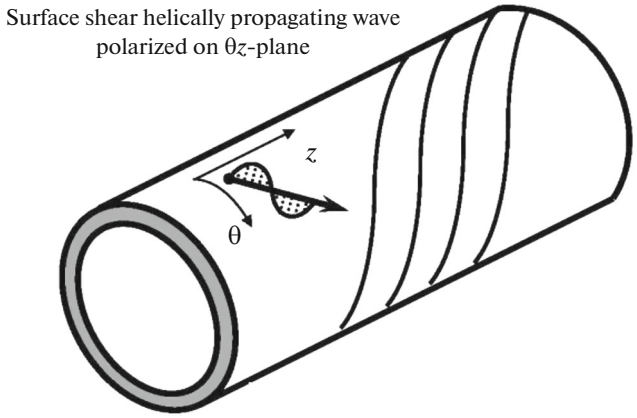

Fig. 9. Shear type wave propagation along the anisotropic cylindrical shell polarized mainly in the principal θz-plane.

ple ($n = 2$) resonance modes illustrate a positive normalized sensitivity (i.e., positive correlation or direct relationship between the variations of the object parameter and the variations of the resonance frequencies) with respect to variations of $\nu_{lt} = \nu_{ls}$, while the 1st and 2nd overtones of the resonance modes (excepting the dipole and quadruple modes of vibration which do not show any sensitivity) depict a negative normalized sensitivity; i.e., negative correlation or inverse relationship between the variations of the object parameter and the variations of the resonance frequencies. In this figure, it is clear that the normalized sensitivity with respect to Poisson ratios is approximately one order smaller than what happens for the other material elastic constants.

CONCLUSIONS

The novel methodology of part 1 of the research work on the wave propagation characteristic of helically wounded cylindrical shells is used to study the wave propagation characteristics of an air-filled and water submerged Graphite/Epoxy cylindrical shell. The singular phenomenon of the resonance bifurcation is unveiled and is tracked in the results of the scattering problem in which the ordinary circumnavigating resonance wave propagation modes (resonance branches) start to doubling as the wave takes a nonzero axial wavelength. Particularly, an attention is paid to the sensitivity analysis of resonances associated with various modes of the wave propagation appearing in the backscattered amplitude to the perturbation in the material constants of composite material. The results illustrated the capability of the resonance spectroscopy technique for non-destructive evaluation of the wounded composite structures.

REFERENCES

1. J.Y. Kim and J.G. Ih, J. App. Acoust. **64**, 1187 (2003).
2. M. Rajabi, Acoust. Phys. **62**(3), (2016) (in press).
3. K.P. Soldatos and J. Ye, J. Acoust. Soc. Am. **96**, 3744 (1994).
4. S.M. Hasheminejad and M. Rajabi, Ultrasonics **47**, 32 (2007).
5. M. Rajabi and S.M. Hasheminejad, Ultrasonics **49**, 682 (2009).
6. M. Rajabi and M. Behzad, Composite Struct. **116**, 747 (2014).
7. M. Rajabi, M.T. Ahmadian, and J. Jamali, Composite Struct. **128**, 395 (2015).